

Quantifying efficient information exchange in real network flows

Giulia Bertagnolli ^{1,2}✉, Riccardo Gallotti ¹ & Manlio De Domenico ¹✉

Network science enables the effective analysis of real interconnected systems, characterized by a complex interplay between topology and network flows. It is well-known that the topology of a network affects its resilience to failures or attacks, as well as its functions. Many real systems—such as the Internet, transportation networks and the brain—exchange information, so it is crucial to quantify how efficiently system’s units communicate. Measures of parallel communication efficiency for weighted networks rely on the identification of an ideal version of the system, which currently lacks a universal definition. Consequently, an inattentive choice might hinder a rigorous comparison of network flows across scales or might lead to a descriptor not robust to fluctuations in the topology or the flows. We propose a physically-grounded estimator of flow efficiency valid for any weighted network, regardless of scale, nature of weights and (missing) metadata, allowing for comparison across disparate systems. Our estimator captures the effect of flows heterogeneity along with topological differences of both synthetic and empirical systems. We also show that cutting the heaviest connections may increase the average efficiency of the system and hence, counterintuitively, a sparser network is not necessarily less efficient.

¹CoMuNe Lab, Fondazione Bruno Kessler, Trento, Italy. ²Department of Mathematics, University of Trento, Trento, Italy. ✉email: gbertagnolli@fbk.eu; mdedomenico@fbk.eu

Complex systems store energy, process and, very often, efficiently exchange information to perform complex tasks. The universal mechanisms behind this behavior are unknown, although pioneering works have shown that the robustness of this type of systems to random failures or targeted attacks¹ might emerge from the trade-off between the cost of exchanging information and the importance of guaranteeing communication dynamics for functioning^{2–4}. Therefore, it is crucial for units in a complex network to route information through shortest paths, broadcasting, or according to some dynamics between these two extremes^{5,6}, as it happens for instance in the Internet⁷. For several applications of interest, even the inverse problem, of identifying either the origin or the destination of the flow from the observation of pathways, is relevant^{8,9}. This framework enables the description of a wide variety of systems, from cell signaling to individuals exchanging information in social/socio-technical systems such as human flows through different parts of a city by public or private transportation means. In the following we focus our attention on flow networks, systems characterized by the exchange of flows—e.g., number of streets between different parts of the city or human movements within a city, migration between different geographic areas, goods traded among countries, packets routed among servers, electricity in a power grid—through edges^{10–13}. System's units and their connections have a limited capacity and, in absence of sources and sinks, the sum of the overall incoming and outgoing flows is constant.

Two descriptors traditionally employed to characterize the structure, and hence indirectly the information flow, of unweighted, simple, sparse, and connected networks are the characteristic path length L and the clustering coefficient C ². L is defined as the average length over all shortest paths in the network, while C is the average local clustering coefficient over all nodes in the network and quantifies the network transitivity. Those networks having both a small characteristic path length L —typical of random graphs—and a large clustering coefficient C —typical of regular lattices—display the so-called “small-world” property², which is found in real world networks and is related to how efficiently the information is exchanged in a system^{3,14}.

One widely accepted measure of efficiency in information flow is the communication efficiency, that has been used to highlight the possible designing principles responsible for neural, man-made communication, and transportation systems³. This measure of efficiency was introduced in 2001³, as a physically grounded and more general way to characterize networks displaying the small-world property. Instead of the two descriptors— L and C —for two apparently different kinds of properties of these networks, the communication efficiency evaluated at different scales is able to identify both structural features, indeed, $1/L$ and C have been shown to be approximations of the efficiency at the global and local scale, respectively. If the clustering coefficient finds a natural, physical generalization in the local communication efficiency, one main difference between the global communication efficiency and the characteristic path length remains: the first concerns the parallel, while the second the sequential information exchange in a system. This discrepancy is negligible if the distances in the network are not too diverse, while it becomes significant if they are highly heterogeneous, as, for instance, in the Internet^{3,14}. A further advantage of the efficiency over the original characterization of small-world networks through L and C , is that it does not require the connectedness and sparseness of the network and, subject to an appropriate normalization, not even its unweightedness.

The topology of a complex network influences the information exchange among its units and is responsible for a rich repertoire of interaction patterns. For instance, the existence of a connection

between two neurons allows them to exchange electrochemical signals and their communication dynamics is relevant for the functional organization of the brain. Similarly, human flows through different geographic areas shape the functional organization of a city and its neighborhood, or even email interactions among individuals in an organization determine how information reaches different teams. In these real systems we never see the everyone-is-connected-to-everyone structure, i.e., fully connected networks, because, even if it would be very efficient for the information exchange, it would also be extremely costly. The trade-off between the communication efficiency and the wiring cost characterizes complex systems and their robustness to perturbation in communication dynamics^{15,16}.

Even more importantly, many empirical systems are characterized by connections with heterogeneous intensities and different correlations among weighted and purely topological network descriptors are ubiquitous¹⁷, from the human brain^{4,18–20} to transportation networks²¹. Therefore, it is essential to account for these underlying weighted architectures to gain real insights about the hidden construction principles and mechanisms used to transform, process, and exchange information¹⁴. An even broader scenario is possible: think for instance at infrastructure systems, where the units do not exchange information in parallel, where communication is subject to queues or priorities, where noise and failures may play an important role in the communication. In this case to assess the efficiency of the system one needs more information that may not be present (or be representable) in the topology or flows of the network.

However, even assuming that information is exchanged in parallel—which is assumed from henceforth so that when we use the terms efficiency or communication efficiency we mean the efficiency of parallel communication—for a wide class of weighted systems¹⁷ which are not embedded in space or for which metadata about the underlying geometry (nodes coordinates) are not available, the normalization of the weighted efficiency descriptor proposed by Latora and Marchiori^{3,14} may fail—due to a mathematical constraint which is not fulfilled—or may be difficult to compute—because of the nature of flows, encoded in edge weights. As a matter of fact, we observed that in many applications^{22–27} the weighted efficiency is not normalized by comparison with the most efficient version of the network at hand, as suggested by Latora and Marchiori^{3,14}, but instead it is computed upon normalized weights. This latter descriptor, to the best of the authors' knowledge, has not yet been studied in detail, so we will take care of it, underlining especially its lack of statistical robustness to fluctuations in the network topology or flows.

In this work we show that a mathematically rigorous, statistically robust, and physically grounded, normalized descriptor of the global efficiency of parallel information exchange can be computed without any knowledge on the system, but its weighted network representation. We demonstrate how to define a suitable “physical distance” between system's units in terms of the flow they exchange across least resistance pathways. We also show that the quantification of the system efficiency might vary dramatically if flows are not adequately accounted for. In fact, discarding edge weights and considering only the topology of a network leads to an overestimation of its communication efficiency. In the opposite direction, incorporating the flows without normalizing the weighted efficiency descriptor leads to a measure that cannot be used to compare different systems. In between these two extremes lie several normalizing procedures for the weighted communication efficiency, which are discussed and compared in the remaining of this article. The normalizing procedures we propose in this work yields an efficiency descriptor that effectively summarizes both the topological and flow information encoded in the

networks; in particular, on synthetic models we observe that the efficiency grows not only when the flows heterogeneity decreases, but also if there is not a subset of privileged pathways monopolizing the whole information flow in the network.

Results

Flow exchange in complex topologies. Let us consider a complex network $G = (V, E)$, whose weighted adjacency matrix $\mathbf{W} = (w_{ij})_{i,j \in V}$ characterizes both its topology—indeed, $w_{ij} = 0$ if i, j are not adjacent, while $w_{ij} > 0$ if they are—and flows—by the magnitude of the weights w_{ij} .

The efficiency ϵ_{ij} in the communication between two nodes $i \neq j \in V$ is assumed to be inversely proportional to their distance d_{ij} ³. It follows that if i and j belong to different connected components, i.e., $d_{ij} = \infty$, $\epsilon_{ij} = 0$. The global communication efficiency of the network G is the average over pairwise efficiencies

$$E(G) = \frac{1}{N(N-1)} \sum_{i \neq j \in V} d_{ij}^{-1}. \quad (1)$$

The natural metric on unweighted networks is the shortest-path distance. In this case the topological distances satisfy $0 \leq d_{ij}^{-1} \leq 1$, implying $0 \leq E(G) \leq 1$, with equality holding when G is a clique and, since each pairwise communication occurs without mediators, information propagates the most efficiently. In case of weighted networks, distances should also account for weights and for what they stand for²⁸. As a matter of fact, the algorithm proposed by Dijkstra in 1959²⁹ (and used mostly) involves the sum of the cost of connections to find the path of least resistance, which means that if the edge weights encode the intensity of interactions, their costs have to be derived before computing weighted distances. Furthermore, weighted distances are real valued so that, in general, $E(G) \in [0, \infty)$ and depends on the scale of the weights. For this reason, a global indicator of efficiency should be rescaled in $[0, 1]$ considering an idealized proxy of G , called G_{ideal} , having maximum efficiency.

In^{3,14} the authors propose to build G_{ideal} based on pairwise physical distances ℓ_{ij} , which are supposed (i) “to be known even if in the graph there is no edge between i and j ”, i.e. $\ell_{ij} > 0$ for all $i \neq j$, (ii) should fulfill the constraint $\ell_{ij} \leq d_{ij}$ for all $i, j \in V$, and (iii) should be considered along with topological information in the computation of weighted shortest-path distances d_{ij} . Then, $E(G_{\text{ideal}}) = \frac{1}{N(N-1)} \sum_{i \neq j \in V} \ell_{ij}^{-1} \geq E(G)$ and $\frac{E(G)}{E(G_{\text{ideal}})}$ —which is henceforth denoted by $\text{GCE}(G)$ —is correctly normalized. For some spatial networks—e.g., transportation systems like the railway or infrastructures such as the power grid—the physical distances are well-defined by the underlying geometry, for others—among which power stations and water resources—it might be difficult to calculate physical distances because of the lack of direct information about spatial coordinates of units. For nonspatial systems—such as social and socio-technical systems— $(\ell_{ij})_{i,j \in V}$ can be found as ad hoc transformations of connection strengths (weights) into connection costs. For instance, in a biological network, where w_{ij} represents the velocity of chemical reaction along a direct connection between i and j , ℓ_{ij} could be taken as its inverse³; or, ℓ_{ij} could be the minimum between 1 and the inverse number of edges between i and j in network with multiple unweighted edges¹⁴. Unfortunately, this apparently straightforward procedure hides several issues, e.g., if there is no direct connection between two biochemical units in a connected network, their physical distance is infinite according to the previous definition, while their weighted shortest-path distance will be some positive real number, violating (ii). Furthermore, in case of real positive weight $w_{ij} \in \mathbb{R}_+$ one cannot take

$\ell_{ij} = \min\left\{1, \frac{1}{w_{ij}}\right\}$, since this introduces a cut-off on weights smaller than 1. We indicate by $E^{\text{LM}} = \frac{E^G}{E(G_{\text{ideal}})}$ the weighted efficiency of G when G_{ideal} is built according to^{3,14}. Another common method for obtaining a normalized efficiency indicator^{22–26}, assuming that the weight encode the interaction intensities, consists in firstly, rescaling the weights into $[0, 1]$, then transforming them to costs (usually taking their reciprocals), applying Dijkstra’s algorithm for evaluating the pairwise distances and finally computing the efficiency by (8), without any further comparison with a G_{ideal} . See the “Methods” section for further details. For instance, let us mention the max-normalization of weights $\tilde{w}_{ij} = \frac{w_{ij}}{\max\{w_{ij}\}}$, which leads to $E^{\text{MN}}(G) = \frac{E(G)}{\max\{w_{ij}\}}$ and will be

used for comparison in the rest of this study. Observe as of now, that this rescaling is particularly sensitive to outliers or extreme values of the link weights and that, differently from the original definition by Latora and Marchiori¹⁴, it compares every pairwise weighted efficiency to the maximum possible efficiency in the whole network. In conclusion, in a broad spectrum of scenarios of practical interest for applications, there is no general recipe to compute $E(G_{\text{ideal}})$.

Rethinking efficiency of information flow in weighted architectures. To overcome the above issues, we build G_{ideal} from the weighted graph G so that physical distances (i) are not necessarily calculated from metadata or accessible spatial information and (ii) preserve a local feature.

We assume hereafter that edge weights are nonnegative real values and represent the strength of connections. Recall that a path is the sequence of vertices in a nonintersecting walk across the network; the length of the path is the number of edges in—or the sum of edge costs along—that path. Weighted shortest-path distances are then computed minimizing the sum of the reciprocals of weights^{30,31}, which can be seen as costs, over all paths between node pairs (other weighted metrics may be used²⁸ but are not discussed here). Let us denote by $\text{SP}(i, j)$ a weighted and possibly directed shortest-path from i to j ; its length, $d_{ij} = \sum_{n,m \in \text{SP}(i,j)} w_{nm}^{-1}$, is the shortest-path distance between i and j , while $\phi_{ij} = \sum_{n,m \in \text{SP}(i,j)} w_{nm}$ is the total flow along $\text{SP}(i, j)$.

The matrix $\Phi = (\phi_{ij})_{i,j \in V}$ represents an artificial connectivity made of shortcuts, where total flows along shortest paths are delivered in one topological step, as shown in Fig. 1. G_{ideal} is then obtained averaging between the true structure \mathbf{W} and the artificial connectivity, i.e., $\mathbf{W}_{\text{ideal}} = \frac{\Phi + \mathbf{W}}{2}$. We finally define $\ell_{ij} = (w_{ij}^{\text{ideal}})^{-1}$ and, hereafter, $\text{GCE}(G)$ indicates the global communication efficiency normalized w.r.t. our G_{ideal} . Note that a stronger option than averaging between the real and the artificial connectivity would be to take $\mathbf{W}_{\text{ideal}} = \Phi$, or to define ϕ_{ij} as the average flow along $\text{SP}(i, j)$.

When G is connected, G_{ideal} is completely connected and ℓ_{ij} is finite $\forall i \neq j$. If otherwise G is not connected, G_{ideal} will be disconnected as well. If there is no path between i, j both $\ell_{ij} = d_{ij} = \infty$ and their pairwise efficiency contribute neither to $E(G)$ nor to $E(G_{\text{ideal}})$. Note that in this case we are computing the average communication efficiency, a global indicator, of disconnected subnetworks, which may not be meaningful. Finally, it is possible to prove (using the Cauchy–Schwarz inequality, see “Methods” section) that the constraint $\ell_{ij} \leq d_{ij} \forall i \neq j$ is always satisfied, hence ℓ_{ij} are well-defined physical distances that can be calculated for any weighted systems. Having defined the mathematical tools, we now analyze some synthetic networks with a tunable structure. This enables us to separate the effects of topology and flows on the global efficiency of the network.

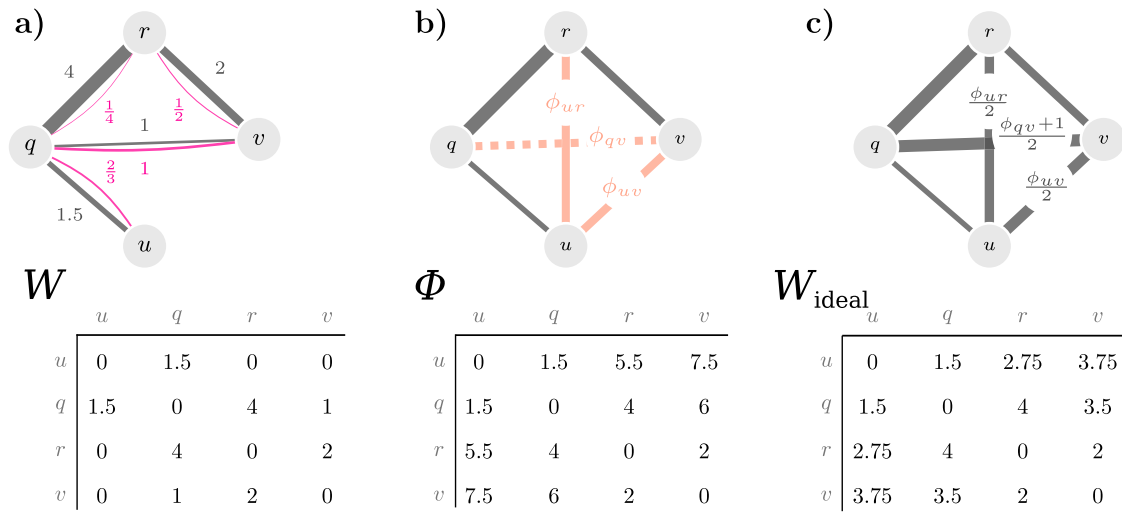


Fig. 1 Computing physically-grounded ideal flows. **a** A simple weighted graph G with four nodes u, q, r and v , link weights in dark gray, and link costs in magenta, and its weighted adjacency matrix \mathbf{W} . Costs are obtained by inverting link weights. **b** The artificial flows added to G and their matrix Φ . **c** G_{ideal} characterized by the weighted adjacency matrix $\mathbf{W}_{\text{ideal}} = \frac{\mathbf{W} + \Phi}{2}$. If the shortest path between two nodes coincides with the edge connecting them, as for u and q , then $\phi_{uq} = w_{uq} = 1.5$ and the edge weight in G_{ideal} is the same as in G . Non adjacent vertices in G (e.g., u, r) have an artificial flow given by the sum of link weights along a shortest paths connecting them ($\phi_{ur} = w_{uq} + w_{qr}$) and in G_{ideal} those vertices are connected by edges with a weight proportional to the artificial flows ($w_{ur}^{\text{ideal}} = \frac{\phi_{ur}}{2} = \frac{1.5+4}{2}$). Finally, there may be pairs of nodes with very weak connections, where topologically longer paths have smaller weighted distances, as for q and v : the cost of the path (q, r, v) is $\frac{1}{4} + \frac{1}{2} = \frac{3}{4} < 1 = \text{“cost of the link } \{q, v\} \text{”}$. In this case the total flow is the sum of the weights along the path (q, r, v) , i.e., $\phi_{qv} = w_{qr} + w_{rv} = 6$ (dashed edge). In G_{ideal} this artificial flow is averaged with the weight of the direct edge $w_{qv}^{\text{ideal}} = \frac{\phi_{qv} + w_{qv}}{2} = 3.5$.

Global efficiency of synthetic networks. We start with the simplest combination of topology and weights: upon a full network (a clique) with $N = 30$ nodes, we generate two ensembles of weighted networks sampling edge weights from different families of probability distributions. The topological efficiency E^T , i.e., (1) with shortest-path distances computed ignoring weights, is 1 for all networks, since they are fully connected. We therefore focus on the weighted descriptors E^{LM} , E^{MN} , and GCE. The trivial case, $w_{ij} = w > 0$ constant, leads to $E^{\text{LM}} = E^{\text{MN}} = \text{GCE} = 1$. We impose more realistic homogeneous flows sampling from a Poisson distribution $\mathcal{P}(\lambda)$ with varying λ . Since zero belongs to the support of the distribution, we add one to each sample to keep the complete connectedness of the network. The heterogeneity in the weighted structure is instead modeled with w_{ij} following power-laws(α) with a lower bound $x_{\min} = 5^{32}$. For each value of the parameters λ and α we take 30 random samples from the respective distribution and generate 30 synthetic weighted networks. Figure 2a) shows their GCEs summarized through boxplots, as a function of λ and α . The five statistics of the GCEs distribution shown in the boxplots are: the first (Q1) and third (Q3) quartiles, or quantiles of order 25 and 75% (resp. lower and upper box hinges)—the width of the box shows the interquartile range ($\text{IQR} = \text{Q3} - \text{Q1}$)—the median (middle line in the box), the smallest observation greater than or equal to $\text{Q1} - 1.5 \cdot \text{IQR}$ (lower whisker) and the largest observation smaller than or equal to $\text{Q3} + 1.5 \cdot \text{IQR}$. Outliers, observations falling outside the expanded IQR are shown as dots. All these synthetic networks are topologically equally efficient since they are fully connected, however, accounting for the weights can lead to dramatically different results. The extreme heterogeneity of edge weights, characteristics of power-law distributions with small scaling exponent, strongly reduces the average communication efficiency of the network. Furthermore, as the tails of the weight distributions become lighter, the weighted GCE tends to the topological one. As the parameters λ and α grow the heterogeneity of weights decreases, since the tailness of the distributions decreases. A measure of the

tailness of a distribution is the kurtosis, the standardized central moment of order 4. Usually, one evaluates the kurtosis minus three, which is called the excess kurtosis, and represents the excess w.r.t. the kurtosis of any normal distribution, which is always equal to three. For the Poisson distribution, the excess kurtosis is λ^{-1} ; for the power-law the excess kurtosis is finite only for $\alpha > 5$ and, for $\alpha > 5$, it decreases as a function of α , tending to 6 as $\alpha \rightarrow \infty$. More details in the Supplementary Note 1. This reduction in the weights distribution tailness can also be seen in Fig. 2b), where we show the probability mass (resp. density) functions for $\lambda = 1, 12$ and $\alpha = 1.5, 7$.

We next study the interplay between weights heterogeneity and topology through bond percolation, i.e., the targeted attack and removal of the links in the network^{26,33}. By removing edges in decreasing weight order, we trim the tail of the weights distributions, reducing their heterogeneity. In Fig. 2c) we plot the four efficiency quantifiers as functions of the fraction f of removed edges and averaged over 30 random realizations of each model. Shaded areas indicate the standard deviation from the mean. We denote by G_f the damaged network obtained from G removing $f\%$ of its heavier links. G_0 is, topologically, a clique, so $E^T(G_0) = 1$. In $E^T(G_f)$ the denominator is always $N(N-1)$, hence G_f is compared with a clique, by definition and $E^T(G_f)$ decreases monotonically. On the other side E^{MN} , E^{LM} (Fig. S4), and GCE use the flows of G_f to build the corresponding G_f^{ideal} and are, consequently non-monotone functions of f . It might seem a limitation nevertheless, it allows us to compare a series of networks G_f with slightly different topologies, increasingly sparser, and flows that become increasingly homogeneous. In the “Methods” section we propose a modification of the GCE to overcome this possible limitation in percolation applications. E^{MN} and GCE behave similarly, although E^{MN} has larger fluctuations because at each step the edge with maximum weight is removed. As expected, there are clear differences in the percolation plots of Poissonian and power-law network flows, but in both cases removing the heaviest links produces an increase in

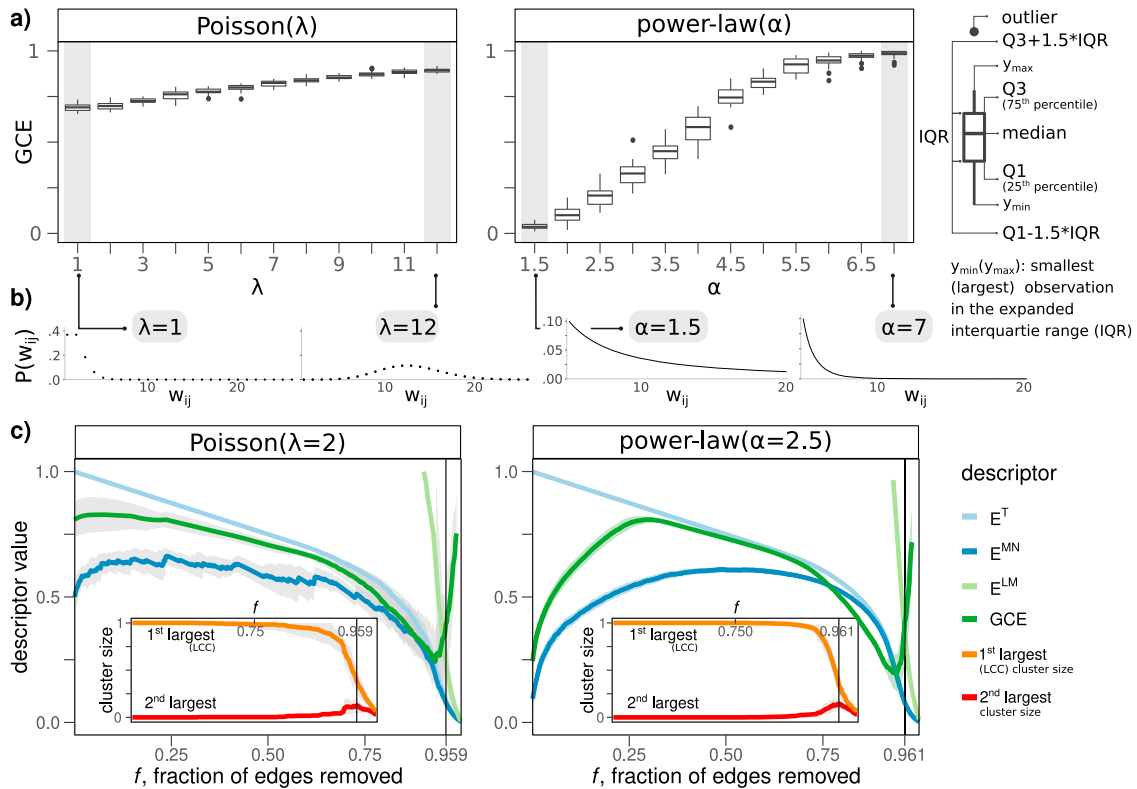


Fig. 2 Communication efficiency of full networks with homogeneous and heterogeneous flows. **a** Global communication efficiency (GCE) as a function of the free parameter λ of the Poisson α and power-law distributions from which flows are simulated. The GCE distribution over 30 networks for each parameter value is summarized by the boxplots. In particular the box extends from the first (Q1) to the third (Q3) quartile, the line in the box indicates the median and the whiskers expand the interquartile range ($IQR = Q3 - Q1$) by ~ 1.5 in each direction (see the legend). As α and λ increase the heterogeneity of the weights decreases and the GCEs tend to 1, the efficiency of a fully connected, unweighted network. For the highlighted values of λ and α , we report the probability mass/density function of edge weights w_{ij} (all nodes are adjacent) in panel **b**. **c** Targeted bond percolation over the same synthetic networks as in **a** for $\lambda=2$ and $\alpha=2.5$. The descriptors are the topological E^T , max-normalized E^{MN} , and Latora-Marchiori E^{LM} efficiency, and our GCE. Lines represent the average descriptor value over the 30 networks, while shaded areas the standard deviations. The average GCE benefits from the removal of heavy links which forces the network to rearrange its paths. The insets show the behavior of the size of the largest and second largest connected component for $f \in [0.5, 1]$. Vertical black lines indicate critical thresholds f_c (corresponding the maximum of the second largest component size). Values on the y axis have been cut to the range $[0, 1]$ —full plot in Fig. S4).

the average communication efficiency. In both cases, when the flows become more homogeneous the GCE depends largely on the topology. Finally, when the network is disrupted—near the critical threshold f_c indicated by the maximum of the second largest component size^{34,35} (insets of Fig. 2)—the GCE has a break-down point, since we are averaging the efficiencies of many, small, distinct (and maybe individually efficient) disconnected networks.

Before moving to synthetic networks with realistic topologies, let us spend few words on the comparison between the GCE and E^{MN} . The latter is, apparently, more attractive than the GCE, because it is easier to compute. A more attentive look, however, reveals some issues: firstly, the sample maximum is the least robust order statistic, i.e., it is very sensitive to extreme values and outliers. If this is not a strong enough reason to avoid it, have a look at Fig. 3. The GCE converges to 1 as the weights become more homogeneous, while E^{MN} remains approximately below 0.5; and these are very specific networks, they are fully connected. What is then the meaning of a descriptor normalized into $[0, 1]$, when the maximum value is so difficult to reach?

Finally, we compare the two descriptors on synthetic networks generated from models of real-systems, in particular small-world networks (Watts–Strogatz (WS) model²) and scale-free networks (Barabási–Albert (BA) model³⁶). Again we consider 30 realizations of each topology, each having $N=256$ nodes, average

degree $\langle k \rangle \simeq 12$ and around 5% of all possible edges. We indicated by $A = (A_{ij})$ the adjacency matrix of each network. Upon these, the edge weights are assigned following the two following rules:

$$w_{ij} = k_i^\beta \quad (2)$$

$$w_{ij} = e_{ij}^\beta \quad (3)$$

where $k_i = \sum_{j=1}^N A_{ij}$ is the degree of node i , e_{ij} is the (topological) edge-betweenness of the link $\{i, j\}$, and β is a free parameter allowing us to tune the flow structure. The betweenness³⁷ of the edge $\{i, j\}$ is the number of the shortest paths between any pairs of nodes s, t that go through $\{i, j\}$, here indicated by g_{sijt} , over the total number of shortest paths between the nodes s and t : $e_{ij} = \sum_{s \neq t} \frac{g_{sijt}}{g_{st}}$. First observe that (2)³⁸ generates asymmetric weights; for positive β hubs have strong out-going links, while for negative values of β the intensity of the connections decreases with the degree. The case $\beta=0$ leads to unweighted systems. Results are summarized in Fig. 4. The poor robustness of E^{MN} emerges in the plot: the distributions of E^{MN} over the ensembles are skewed and have greater variance. Therefore, we focus on the GCE for the between models comparison. Topologically, BA networks are slightly more efficient than WS networks, but as soon as weights are introduced the panorama changes: the degree distribution of small-world networks is less heterogeneous w.r.t.

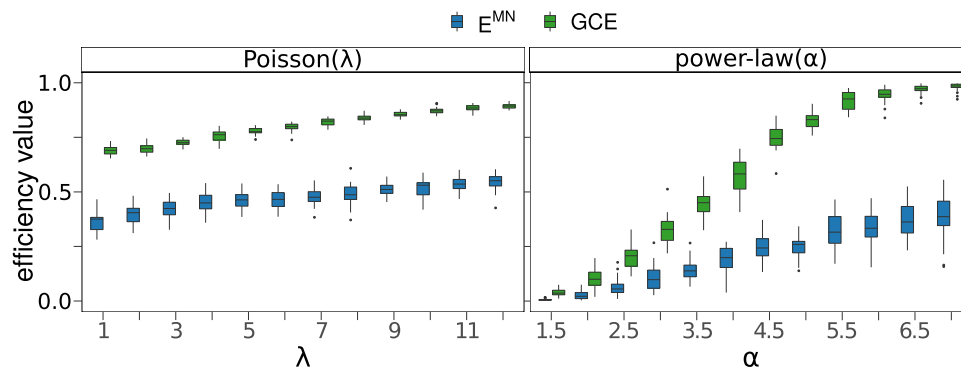


Fig. 3 Comparison of weighted efficiency descriptors for full networks with homogeneous and heterogeneous flows. The descriptors are the global communication efficiency GCE and the max-normalized efficiency E^{MN} . For each parameter value the GCE and E^{MN} are evaluated for 30 synthetic networks and their distributions are summarized through boxplots. The five statistics in the boxplots are: the first (Q1) and third (Q3) quartiles, or quantiles of order 25 and 75% (resp. lower and upper box hinges), the median (middle line in the box), the whiskers extend from the smallest to the largest observation in the range $[Q1 - 1.5 \cdot (Q3 - Q1), Q3 + 1.5 \cdot (Q3 - Q1)]$. Observations falling outside this range are outliers, shown as dots. The GCE converges to 1 as the heterogeneity of the weights distributions decreases (i.e., as λ and α increase), while E^{MN} remains approximately below 0.5.

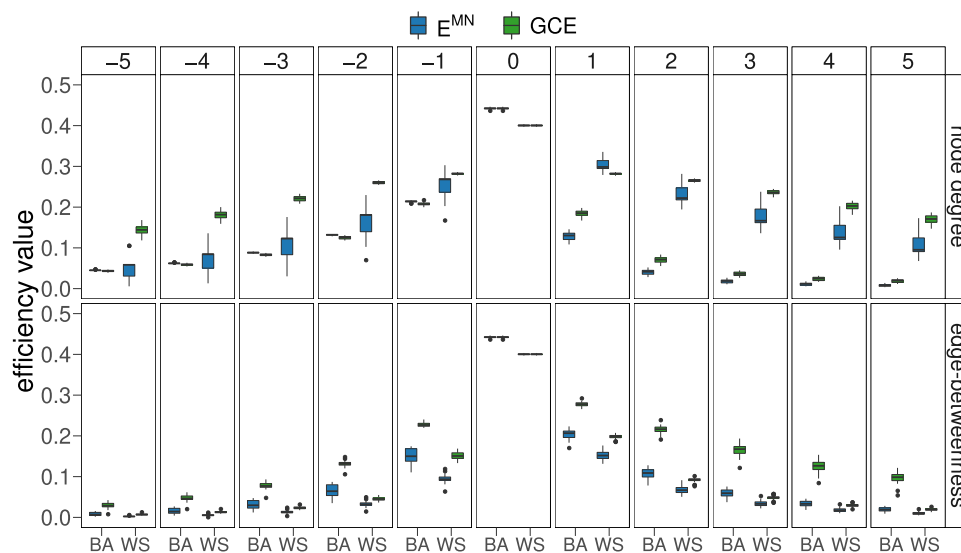


Fig. 4 Comparison of weighted efficiency descriptors for synthetic networks with different topologies and flows. Topologies are generated from the Barabasi-Albert (BA) and Watts-Strogatz (WS) models while flows are generated according to (2) and (3) for varying $\beta \in [-5, 5]$ as specified at the top of each column. The parameter β controls the agreement—direct (inverse) proportionality for $\beta \geq 0$ ($\beta < 0$)—between the outgoing strength of the nodes and their degree (in the plot labeled “node degree”) and between the weight of edges and their edge-betweenness (in the plot labeled “edge-betweenness”). The descriptors are the global communication efficiency GCE and the max-normalized efficiency E^{MN} . See Fig. 2 for the detailed legend of boxplots.

the scale-free leading to less heterogeneous weights generated by (2) and higher efficiency, independently from the sign of β . On the other side, when links strengths are related to their topological betweenness, BA networks are generally more efficient than WS networks and when $\beta > 0$ the networks are more efficient, because those edges that are very in-between shortest paths are also very efficient. Notice that here, differently from the previous example where all possible links were present, communication paths are unlikely to be able to “reorganize” (i.e., choose a different sequence of edges) in response to weights changes.

Global efficiency of real interconnected systems. We use our framework to study the efficiency of four real systems (see Table 1). From the FAO worldwide food trade network we selected the layers of cocoa, coffee, tea, and tobacco. From the migration dataset we selected internal migration flows inside three Asian regions: India, China, and Vietnam. From the worldwide air traffic network we extracted the traffic in and between Europe and

Africa. Finally, we consider the structural connectivity of human brain, quantified through diffusion tensor imaging (DTI) and fiber tractography methods.

These real networks have different properties, among which edge density and weight distribution. Based on the results of our analysis of synthetic networks and on previous studies^{14,26}, we expect the weighted efficiency of these real networks to be smaller than their topological efficiency. Thanks to our normalizing procedure, which can be applied unchanged to all networks, it is legitimate to compare the weighted efficiencies of diverse systems and we expect the trade networks to have the smallest efficiency. As a matter of fact, observing the boxplots in Fig. 5 (and Fig. S8 of the Supplementary Note 2) we can see that the distributions of the network flows in the trade networks are highly heterogeneous. The whiskers in the boxplots extend from the minimum to the maximum of the distribution to highlight the presence of extreme outliers or very heavy tails. Let us then look at the results of the analysis.

Table 1 Real-world flow networks and corresponding scales.				
Dataset		V	E	Ref.
FAO	cocoa	159	2081	39
	coffee	184	7760	
	tea	172	3297	
	tobacco	183	3623	
Migrations	China	30	870	40,41
	India	32	992	
	Vietnam	63	3906	
Transportation	airports	299	12,919	43
Biological	human brain	188	10,836	42

[V] indicates the number of nodes and [E] the number of edges in the networks. Multiple edges have been aggregated and loops removed.

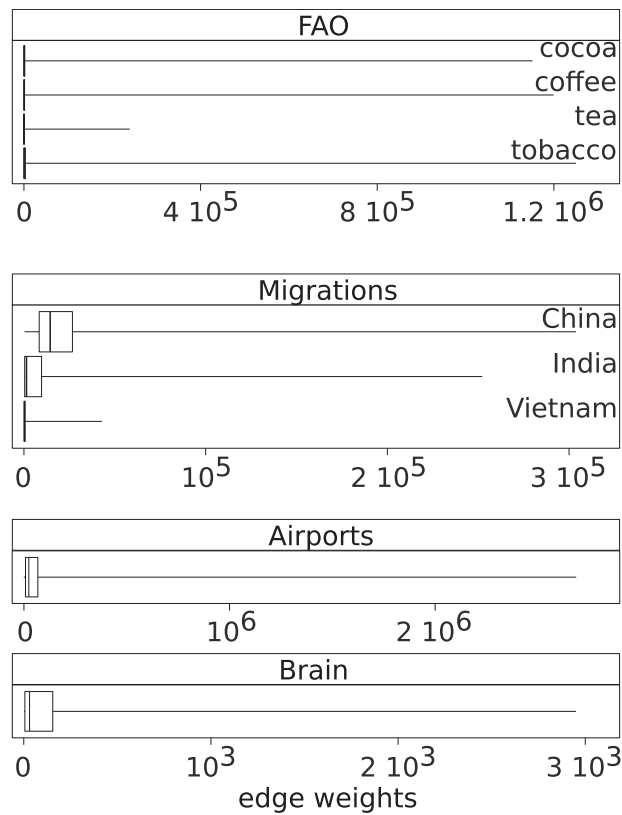


Fig. 5 Edge weights distributions of selected real-world networks. The number of nodes and edges of each network is specified in Table 1. Heterogeneity and scale vary across the datasets. The statistics of the boxplots are the first and third quartiles of the weights distribution are displayed as the lower and upper hinges of the box, the line in the box represents the median, whiskers extend from the minimum to the maximum weight.

Figure 6 shows the curves corresponding to $E^T(G_f)$ and $GCE(G_f)$. Independently from the system, ignoring the network flows leads to an overestimation of the average efficiency, especially when flows are highly heterogeneous. The network of internal migration, is the most efficient, but it also has the highest cost being a clique. The tea trade network is the most inefficient. Finally the brain and the airports network have similar GCEs until the first 25% of their edges are removed, with the brain remaining afterwards more efficient w.r.t the reduced flows. Observe that the total flow could be restored, while keeping a specific efficiency value, redistributing the removed flow on the

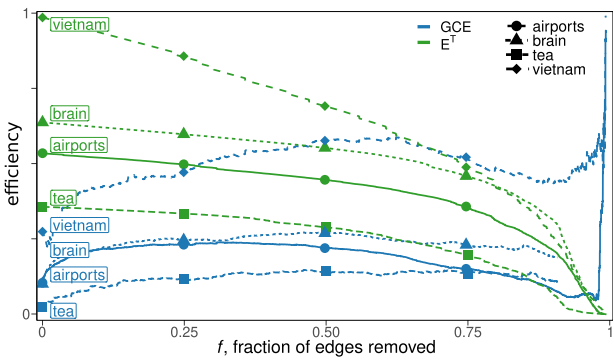


Fig. 6 Targeted bond percolation of real interconnected systems. The descriptors are the topological efficiency E^T and the global communication efficiency GCE of real networks where edges are removed in decreasing order according to their weight. The networks are: The tea trade network, the internal migrations in Vietnam, the air traffic between airports in Europe and Africa, and the human brain network. See also Figs. S9 and S10 in the Supplementary Note 2.

remaining links. In general, removing those edges monopolizing shortest paths forces their reallocation inducing an increase of the global weighted efficiency.

Conclusion

Exchanging information is one of the main functions of many real complex systems and quantifying how efficiently they perform this task is of great interest for different disciplines. Consequently, the concept of communication and transport efficiency is relevant for a broad range of applications, from public transportation to the human brain and the Internet. Defining the efficiency and telling which system is efficient from which is not, is still an open and debated question. It depends on the context —“Are we interested in the efficiency of a system in relation to an objective, such as a maximum cost, a performance level, or in an absolute efficiency measure?”—on the amount of information available on the system—“Do its units have to wait before passing a message?”, “Is this information encoded (or even, can this information be encoded) in the network representing the system?”—etc. For instance, communication and transport processes in many real systems may involve waiting times, error rates and technical inefficiency of the networked system, and possibly, also other variables that cannot be encoded as purely topological network features. In this case, characterizing the efficiency of the system by link weights and weighted shortest-path distances is an oversimplification.

However, given a network, without any metadata, we can reasonably assume that nodes connected by a link are closer or more similar than disconnected nodes, and that connected nodes communicate more easily and efficiently than disconnected ones. Furthermore, we can assume that strong, heavy links bring the nodes nearer, reducing the cost of their interaction and communication. Hence, our approach on system’s efficiency is based on the assumptions (i) of parallel information exchange between units and (ii) that the network representation of the system is enough for assessing its communication efficiency. Under these assumptions, we studied systems represented by flow networks, where links encode volumes of people, electrochemical junctions, packets, etc. While there is a widely adopted descriptor for the global communication efficiency in case of unweighted networks, we have found that its generalization to the case of weighted networks might not be suitable in all relevant cases. In this work we have identified and explained the mathematical limitations of the current measures.

A direct consequence of our analysis is that an estimation of global efficiency can be trusted only under specific conditions: i.e., the analysis of efficiency in the case of real network flows cannot be performed or, alternatively, when it is performed it might lead to important underestimation or overestimation of results, which agrees with previous results²⁶. Since flow networks are ubiquitous, here we have proposed the most general definition of the global communication efficiency for weighted directed networks, which does not assume any other (meta-)information on the system.

Using our physically grounded definition of flow network efficiency, our results indicate that one can achieve a desired level of efficiency by wisely redistributing weights, instead of altering the underlying topology. This result is relevant for practical applications, since it is not always guaranteed that one can rewire or dramatically change with other interventions the network connectivity. In fact, altering network structure is usually expensive in economic or energetic terms. Our framework works under mild assumptions about the underlying topology and about the ideal and most efficient network, with no metadata, nor additional spatial (e.g., geographic) information on the system, allowing for trustworthy applications to empirical problems. It also allows for a complementary view of bond percolation from a functional perspective, allowing us to gain new insights about critical phases of information exchange and network flows in addition to topological ones.

Methods

Mathematical details on the normalizing procedure. We provide the proof of $d_{ij} \geq \ell_{ij} \forall i \neq j \in V$, which is a sufficient condition for the GCE to be correctly normalized in $[0, 1]$. Recall that $SP(i, j)$ denotes a weighted (directed) shortest-path from i to j and $d_{ij} = \sum_{n \in SP(i, j)} w_{nm}^{-1}$. Observe also that, if the shortest-path between i, j coincides with their link (i, j) the number of vertices in the sequence is $|SP(i, j)| = 2$ and their shortest-path distance is $d(i, j) = \frac{1}{w_{ij}}$. The total flow between i and j through the shortest-path $SP(i, j)$ is defined as $\phi_{ij} = \sum_{n \in SP(i, j)} w_{nm}$.

Before proving our main statements we write an inequality, which will be extensively used in the following proofs. The Cauchy-Schwarz inequality for vectors \mathbf{u}, \mathbf{v} in an inner product space reads $|\langle \mathbf{u}, \mathbf{v} \rangle|^2 \leq \langle \mathbf{u}, \mathbf{u} \rangle \cdot \langle \mathbf{v}, \mathbf{v} \rangle$. Taking $\mathbf{u} = (\frac{1}{\sqrt{x_1}}, \dots, \frac{1}{\sqrt{x_n}})$ and $\mathbf{v} = (\sqrt{x_1}, \dots, \sqrt{x_n})$ the inequality becomes

$$\begin{aligned} n^2 &= \left(\sum_{i=1}^n \frac{\sqrt{x_i}}{\sqrt{x_i}} \right)^2 \leq \left(\sum_{i=1}^n \frac{1}{\sqrt{x_i}} \right) \left(\sum_{i=1}^n x_i \right) \\ n^2 \left(\sum_{i=1}^n x_i \right)^{-1} &\leq \left(\sum_{i=1}^n \frac{1}{x_i} \right). \end{aligned} \quad (4)$$

(4) states that for nonnegative real numbers x_1, \dots, x_n the inverse of their sum is smaller or equal to the sum of their reciprocals.

Since we have assumed edges weights to be positive we can apply the inequality, which leads us to

$$\left(\sum_{n \in SP(i, j)} w_{nm} \right)^{-1} \leq |SP(i, j)|^2 \left(\sum_{n \in SP(i, j)} w_{nm}^{-1} \right)^{-1} \leq \sum_{n \in SP(i, j)} w_{nm}^{-1}. \quad (5)$$

Observe that $|SP(i, j)| \geq 2$ if G is connected, therefore the first inequality is actually strict.

From (5) we can derive useful inequalities involving $w_{ij}, \phi_{ij}, d_{ij}$ and ℓ_{ij} :

$$\phi_{ij}^{-1} = \left(\sum_{n \in SP(i, j)} w_{nm} \right)^{-1} \leq \sum_{n \in SP(i, j)} w_{nm}^{-1} = d_{ij} \quad (6)$$

note that if $w_{ij} \neq 0$, it also holds $d_{ij} \leq \frac{1}{w_{ij}}$.

It is also possible to prove that $\phi_{ij} \geq w_{ij} \forall i, j \in V$. Indeed, if i, j are not adjacent then $w_{ij} = 0$ but, since G is connected, there is a path between them with $\phi_{ij} > 0$. If instead, they are adjacent, either $\phi_{ij} = w_{ij}$ meaning that the weighted shortest-path coincides with the edge (i, j) , or there is a shortest-path going through other vertices, such that $d_{ij} = \sum_{n \in SP(i, j)} w_{nm}^{-1} < \frac{1}{w_{ij}}$ and the claim follows from (6).

Starting from the definition of physical distances ℓ_{ij} , using simple inequalities and (5)

$$\begin{aligned} \ell_{ij} &= 2(w_{ij} + \phi_{ij})^{-1} \leq 2 \left(\sum_{n \in SP(i, j)} w_{nm} \right)^{-1} \leq |SP(i, j)|^2 \left(\sum_{n \in SP(i, j)} w_{nm} \right)^{-1} \\ &\leq \sum_{n \in SP(i, j)} w_{nm}^{-1} = d_{ij}. \end{aligned} \quad (7)$$

Again, for a connected network G the strict inequality $\ell_{ij} < d_{ij}$ holds.

Finally, $\phi_{ij} = 0$ if and only if i and j lie in disconnected components and, consequently, the ideal network is disconnected as the original one. In this case both $d_{ij} = \frac{1}{\phi_{ij}} = \infty$ and the missing links among disconnected components will not produce an underestimation of the efficiencies of the subgraphs. Of course, if the network is very fragmented, the GCE, a global descriptor, will not be very informative. Below, we propose a variant of the GCE, which is most appropriate in this case and in percolation simulations in general.

Comparisons with other weighted efficiency measures. In this work we introduced existing measures of topological and weighted efficiency, more specifically, E^T the topological efficiency defined in³, E^{LM} defined by Latora and Marchiori in ref. ¹⁴, E^{MN} obtained evaluating the efficiency on the network with max-normalized weights.

Let us recall the definition of efficiency³

$$E(G) = \frac{1}{N(N-1)} \sum_{i \neq j \in V} d_{ij}^{-1}. \quad (8)$$

where we have the sum of the reciprocal values of pairwise distances $\sum_{i \neq j \in V} d_{ij}^{-1}$ divided by the number of non-diagonal entries in the distances matrix, i.e., $N(N-1)$. In the topological case this last term plays the role of a normalizing factor, since the sum of inverse shortest-path distances in a clique is exactly equal to $N(N-1)$. We refer to the efficiency (8) evaluated without edge weights, or in other words with topological shortest-path distances (d_{ij}), as the topological efficiency and indicate it by E^T . Then E^T naturally lies in $[0, 1]$.

The main difficulty arising in the definition of a weighted efficiency descriptor, have to do with the diversity of information that can be encoded as edge weights in a network. Usually weights represent connection strengths and connection costs are obtained as a function (e.g., inverse) of weights. Given the connection costs, one can compute weighted shortest-path distances²⁸⁻³¹, which vary in $[0 + \infty]$ and therefore, the efficiency computed according to (1) $E(G) \in [0 + \infty]$ and needs to be rescaled (or normalized) in order to be comparable among different systems.

E^{MN} , which has been used, for instance, in refs. ^{22,24-26} is the simplest generalization of E^T to the weighted case: rescaling the weights to $[0, 1]$ implies that shortest-path distances $d_{ij} \geq 1$, since weighted shortest paths are those paths minimizing the sum of edge costs, that is, inverse weights. Consequently, being $d_{ij} \geq 1$, (8) results to be normalized. Different rescaling transformations of weights are possible, the most common is the max-normalization (from which the superscript MN) $\tilde{w}_{ij} = \frac{w_{ij}}{\max_{ij} w_{ij}}$. The cost of edges is then \tilde{w}_{ij}^{-1} . We show, now, that

$E^{MN}(G) = \frac{E(G)}{w_{\max}}$, where $E(G)$ is (8) calculated on weighted geodesic distances without the max-normalization of weights. Let w_{\max} be the maximum weight over all edges of a weighted network $G = (V, E)$ and let $SP(i, j)$ be a weighted shortest path between $i, j \in V$. Observe that the max-normalization of weights does not affect the shortest path, but it does affect the shortest-path distance

$$\tilde{d}_{ij} = \sum_{n \in SP(i, j)} \frac{1}{\tilde{w}_{ij}} = \sum_{n \in SP(i, j)} \frac{w_{\max}}{w_{ij}} = w_{\max} d_{ij}.$$

Finally,

$$E^{MN}(G) = \frac{1}{N(N-1)} \sum_{i \neq j \in V} \tilde{d}_{ij}^{-1} = \frac{1}{w_{\max}} E(G).$$

This fact, could be appealing for computational reasons, but it is definitely not from a statistical point of view: the sample maximum and minimum are the least robust statistics, they are maximally sensitive to outliers. For this reason E^{MN} may have very wild fluctuations over topologically similar networks but with different maximum weights, which makes this indicator not well suited for comparisons between different systems. To make it clearer, using this descriptor you might not be able to tell if your systems show different global efficiency values because they are characterized by different topologies and interplay between topology and flows, or because their maximum weights are, or are not, outliers to their weights distributions, a very global and extreme feature of the network. Of course, not only the max-normalization and inverse are available, for instance, in ref. ²³ weights are wavelet correlation coefficient between regions in the brain and the cost of the connection between regions i and j is defined as $c_{ij} = 1 - w_{ij}$.

E^{LM} is the weighted generalization of $E(G)$ proposed by Latora and Marchiori in ref. ¹⁴. The idea is to normalize $E(G)$ considering an ideal case G_{ideal} where all possible edges are present in the idealized graph and the information propagated

most efficiently. Then,

$$\frac{E(G)}{E(G_{\text{ideal}})} = \frac{\frac{1}{N(N-1)} \sum_{i \neq j \in V} d_{ij}^{-1}}{\frac{1}{N(N-1)} \sum_{i \neq j \in V} \ell_{ij}^{-1}} \leq 1. \quad (9)$$

Observing that a sufficient condition for (9) is $0 \leq \ell_{ij} \leq d_{ij}$ for all $i, j \in V$, defining G_{ideal} reduces to building the matrix $(\ell_{ij})_{i,j}$. They called ℓ_{ij} physical distances, in contrast to shortest-path distances, highlighting that the latter are computed using “the information contained both in the binary adjacency matrix and in $(\ell_{ij})_{i,j}$ ”. Observe that the matrix $(\ell_{ij})_{i,j}$ is, in every respect, a matrix of connection costs. In ref. ¹⁴ (Sec. 3) the authors give some examples to ℓ_{ij} from edge weights. For instance, if weights $w_{ij} \geq 1$ one can define $\ell_{ij} = \min\{1, \frac{1}{w_{ij}}\}$, which is the transformation adopted in this work to compute E^{LM} .

We refer to the Supplementary Note 2 (Figs. S2 and S3) for the full plot corresponding to Fig. 2b) of this study. The GCE converges faster to 1 as the weight distributions become less heterogeneous (in terms of kurtosis). We claim that the maximum of the GCE is obtained not only for full networks with constant edge weight distribution, but it is sufficient to have a uniform edge betweenness, as shown in Fig. S3.

Finally, the panel c) of Fig. 2 without the cut on the range of γ – values is reported in Fig. S4 of the Supplementary Note 2. The percolation simulation consists in removing edges from an undirected weighted full network G , in decreasing weight order. We indicate by f the fraction of edges removed from G and by G_f the resulting, damaged, network with $G_0 = G$. We then evaluate the efficiency of G_f by means of the already described measures: E^T , E^{MN} , E^{LM} , and GCE. We repeat the process 30 times, sampling the edge weights from a Poisson distribution with parameter $\lambda = 2$ and 30 times, sampling the edge weights from a power-law distribution with free parameter $\alpha = 2.5$. We include also the plots for common percolation indicators, such as the total weight of—i.e., the sum of the weights in—the largest connected component (LCC) rescaled in $[0, 1]$, the size of the second LCC—divided by $N = |V|$ —and the number of clusters (components)—also divided by $N = |V|$; see Fig. S5. The second LCC size has proven better at pinpointing the critical threshold in percolating lattices³⁵, as well as at distinguishing between percolation regimes³⁴.

Our normalization procedure can also be used to build a slightly modified version of the GCE that plays the role of a weighted integrity descriptor for percolation analysis. Let G_0^{ideal} be the idealized network corresponding to G_0 build as described in our study. Then

$$\text{GCE}^*(G_f) = \frac{E(G_f)}{E(G_0^{\text{ideal}})} \quad (10)$$

is normalized in $[0, 1]$ and it is a monotone decreasing function w.r.t. f .

This variant of the GCE has been evaluated for real networks in the Supplementary Note 2, Fig. S9.

On artificial flows. We choose to build the artificial flows integrating weights over paths, but this is not the only possibility, provided that constraint $\ell_{ij} \leq d_{ij}$ is satisfied. Now, using the same definitions and notation adopted in this study,

$$d_{ij} = \sum_{n, m \in \text{SP}(i, j)} \frac{1}{w_{nm}} \geq \frac{1}{\min\{w_{nm} : n, m \in \text{SP}(i, j)\}} \quad (11)$$

$$\geq \frac{|\text{SP}(i, j)|}{\sum_{n, m \in \text{SP}(i, j)} w_{nm}} \quad (12)$$

$$\geq \frac{1}{\max\{w_{nm} : n, m \in \text{SP}(i, j)\}} \quad (13)$$

$$\geq \frac{1}{\phi_{ij}}$$

So both the minimum, the maximum, and the average weight over the path are valid choices, as well as, the sum (our choice) and the maximum over all edges (the already discussed max-normalization). Now, when using the sum of flows over paths, we can combine the two sources of information \mathbf{W} and Φ through the arithmetic mean, while this strategy is not possible if we define $\phi_{ij}^* = \min\{w_{nm} : n, m \in \text{SP}(i, j)\}$ (resp. max) because we cannot prove that $\ell_{ij} = \frac{2}{\phi_{ij}^* + w_{ij}} \leq d_{ij}$, so we should drop \mathbf{W} and simply define $\mathbf{W}_{\text{ideal}} = \Phi^*$. We implemented these choices corresponding to the minimum and maximum and show the results on our synthetic networks ensembles in Fig. S6. The two variants, called here GCE^{min} , GCE^{max} , converge faster to 1, since both minimizations (11)–(13) are less strict than ours (the sum). Taking the minimum (11), in particular, may result in values of efficiency spanning a narrow range, near 1, with a consequent difficulty in distinguishing networks on the basis of efficiency. Furthermore, in the bottom panel of Fig. S6 we can see a decreasing-increasing behavior of GCE^{min} which is,

from our point of view, not desirable. GCE^{max} displays, in general, a larger variability. We opt for the sum, since it has a physical meaning in terms of total flow of a subgraph (a path $\text{SP}(i, j)$), it allows us to average the artificial flows matrix with the original flows given by \mathbf{W} and, last but not least, it is easily worked with in mathematical terms (simplifies rigorous proofs).

On the normalized weighted efficiency of Latora and Marchiori¹⁴. Let us take G as the subgraph consisting of vertices q, r, v of Fig. 1 (indicated now by the indices $\{1, 2, 3\}$) and suppose that the weights are the result of the aggregation of multiple binary connections. Its weighted adjacency matrix is

$$\mathbf{W} = \begin{pmatrix} \cdot & 4 & 1 \\ 4 & \cdot & 2 \\ 1 & 2 & \cdot \end{pmatrix}$$

We can compute physical distances ℓ_{ij} following the suggestions in ref. ¹⁴ and shortest-path distances d_{ij} minimizing the sum of costs (i.e., inverse weights)

$$\mathbf{L} = \begin{pmatrix} \cdot & \frac{1}{4} & 1 \\ \frac{1}{4} & \cdot & \frac{1}{2} \\ 1 & \frac{1}{2} & \cdot \end{pmatrix} \quad \mathbf{D} = \begin{pmatrix} \cdot & \frac{1}{4} & \frac{3}{4} \\ \frac{1}{4} & \cdot & \frac{1}{2} \\ \frac{3}{4} & \frac{1}{2} & \cdot \end{pmatrix}.$$

The global communication efficiency defined in ref. ¹⁴ is given by $E^{\text{LM}} = \frac{E(G)}{E(G_{\text{ideal}})}$, where $E(G) = \frac{1}{N(N-1)} \sum_{i \neq j} \frac{1}{d_{ij}}$ and $E(G_{\text{ideal}}) = \frac{1}{N(N-1)} \sum_{i \neq j} \frac{1}{\ell_{ij}}$. Observe that the condition (which is sufficient for $\frac{E(G)}{E(G_{\text{ideal}})} \leq 1$)

$$d_{ij} \geq \ell_{ij} \quad \forall i \neq j \in V \quad (14)$$

is not satisfied for $i = 1, j = 3$ and this causes $\text{GCE} = \frac{E(G)}{E(G_{\text{ideal}})} = \frac{22}{9} \left(\frac{2}{3}\right)^{-1} > 1$.

This counter-example on the statement of (14) is not a pathological case: (14) is violated whenever the weighted shortest-path between adjacent nodes i, j does not traverse the direct link e_{ij} , i.e., $d_{ij} < \frac{1}{w_{ij}}$ and it may often happen in real networks with large heterogeneous weights.

Trying to reproduce the results in ref. ¹⁴, we considered the neural network of the *C. elegans*^{2,14}, with data from <http://www-personal.umich.edu/mejn/netdata/>. Firstly, we aggregate multiple edges, obtaining a simple, directed, weighted network with $N = 297$ nodes, $m = 2345$ edges, and weights in the range $[1, 70]$. If we consider the network as undirected, we obtain $m = 2148$ edges and weights in the range $[1, 72]$. The data are not the same used in ref. ¹⁴, so we cannot reproduce their results exactly. Let us focus on the undirected network: Fig. S7 shows the distance matrix \mathbf{D} evaluated using Dijkstra's algorithm with the reciprocal of edge weights, and the matrix of physical distances \mathbf{L} , with $\ell_{ij} = \min\{1, \frac{1}{w_{ij}}\}$.

Real interconnected systems, additional results. Here we first apply the variant of the GCE, i.e., $\text{GCE}^*(G_f)$ to the networks of migrations inside Vietnam and of the human brain; secondly, we report the detailed percolation results for the real network flows discussed in this study.

We refer to the Supplementary Note 2, Fig. S9, to show the behavior of $\text{GCE}^*(G)$ for two of the real networks from Table 1.

Finally, we show the percolation plots for the remaining datasets studied in this work, see Supplementary Figs. S11 and S12.

Data availability

The datasets generated during the current study are available from the corresponding authors on reasonable request. The real networks data are publicly available through the corresponding references^{39–42}. The worldwide air-transportation flow data⁴³ has been provided by Dirk Brockmann upon request.

Code availability

The custom code that supports the findings of this study is available at the following github repository: [gbertagnolli/efficiency-networks](https://github.com/gbertagnolli/efficiency-networks) or from the corresponding authors on reasonable request.

Received: 10 August 2020; Accepted: 27 April 2021;

Published online: 09 June 2021

References

- Albert, R., Jeong, H. & Barabási, A.-L. Error and attack tolerance of complex networks. *Nature* **406**, 378 (2000).
- Watts, D. J. & Strogatz, S. H. Collective dynamics of ‘small-world’ networks. *Nature* **393**, 440 (1998).
- Latora, V. & Marchiori, M. Efficient behavior of small-world networks. *Phys. Rev. Lett.* **87**, 198701 (2001).

4. Avena-Koenigsberger, A., Misić, B. & Sporns, O. Communication dynamics in complex brain networks. *Nat. Rev. Neurosci.* **19**, 17 (2018).
5. Yan, G., Zhou, T., Hu, B., Fu, Z.-Q. & Wang, B.-H. Efficient routing on complex networks. *Phys. Rev. E* **73**, 046108 (2006).
6. Rocks, J. W., Liu, A. J. & Katifori, E. Hidden topological structure of flow network functionality. *Phys. Rev. Lett.* **126**, 028102 (2021).
7. Huijtema, C. *Routing in the Internet* (Prentice-Hall, 2000).
8. Goltsev, A. V., Dorogovtsev, S. N., Oliveira, J. G. & Mendes, J. F. Localization and spreading of diseases in complex networks. *Phys. Rev. Lett.* **109**, 128702 (2012).
9. Pinto, P. C., Thiran, P. & Vetterli, M. Locating the source of diffusion in large-scale networks. *Phys. Rev. Lett.* **109**, 068702 (2012).
10. Lima, A., De Domenico, M., Pejović, V. & Musolesi, M. Disease containment strategies based on mobility and information dissemination. *Sci. Rep.* **5**, 10650 (2015).
11. Rosvall, M., Esquivel, A. V., Lancichinetti, A., West, J. D. & Lambiotte, R. Memory in network flows and its effects on spreading dynamics and community detection. *Nat. Commun.* **5**, 1–13 (2014).
12. Li, D. et al. Percolation transition in dynamical traffic network with evolving critical bottlenecks. *Proc. Natl Acad. Sci. USA* **112**, 669–672 (2015).
13. Arianos, S., Bompard, E., Carbone, A. & Xue, F. Power grid vulnerability: a complex network approach. *Chaos* **19**, 013119 (2009).
14. Latora, V. & Marchiori, M. Economic small-world behavior in weighted networks. *Eur. Phys. J. B Condens. Matter Complex Syst.* **32**, 249–263 (2003).
15. Hens, C., Harush, U., Haber, S., Cohen, R. & Barzel, B. Spatiotemporal signal propagation in complex networks. *Nat. Phys.* **15**, 403–412 (2019).
16. Harush, U. & Barzel, B. Dynamic patterns of information flow in complex networks. *Nat. Commun.* **8**, 1–11 (2017).
17. Barrat, A., Barthélemy, M., Pastor-Satorras, R. & Vespignani, A. The architecture of complex weighted networks. *Proc. Natl Acad. Sci. USA* **101**, 3747–3752 (2004).
18. Bullmore, E. & Sporns, O. Complex brain networks: graph theoretical analysis of structural and functional systems. *Nat. Rev. Neurosci.* **10**, 186 (2009).
19. Bassett, D. S. & Sporns, O. Network neuroscience. *Nat. Neurosci.* **20**, 353 (2017).
20. van den Heuvel, M. P. & Sporns, O. A cross-disorder connectome landscape of brain dysconnectivity. *Nat. Rev. Neurosci.* **20**, 435–446 (2019).
21. Latora, V. & Marchiori, M. Is the Boston subway a small-world network? *Phys. A* **314**, 109–113 (2002).
22. Rubinov, M. & Sporns, O. Complex network measures of brain connectivity: uses and interpretations. *Neuroimage* **52**, 1059–1069 (2010).
23. Achard, S. & Bullmore, E. Efficiency and cost of economical brain functional networks. *PLoS Comput. Biol.* **3**, 1–10 (2007).
24. Bullmore, E. T. & Bassett, D. S. Brain graphs: graphical models of the human brain connectome. *Annu. Rev. Clin. Psycho.* **7**, 113–140 (2011).
25. Watson, C. G. brainGraph: graph theory analysis of brain MRI data. *R package version 2.7.3* CRAN.R-project.org/package=brainGraph (2019).
26. Bellingeri, M., Bevacqua, D., Scotognella, F. & Cassi, D. The heterogeneity in link weights may decrease the robustness of real-world complex weighted networks. *Sci. Rep.* **9**, 1–13 (2019).
27. van den Heuvel, M. P. & Sporns, O. Rich-club organization of the human connectome. *J. Neurosci.* **31**, 15775–15786 (2011).
28. Opsahl, T., Agneessens, F. & Skvoretz, J. Node centrality in weighted networks: Generalizing degree and shortest paths. *Soc. Netw.* **32**, 245–251 (2010).
29. Dijkstra, E. W. A note on two problems in connexion with graphs. *Numerische Mathematik* **1**, 269–271 (1959).
30. Newman, M. E. Scientific collaboration networks. ii. shortest paths, weighted networks, and centrality. *Phys. Rev. E* **64**, 016132 (2001).
31. Brandes, U. A faster algorithm for betweenness centrality. *J. Math. Sociol.* **25**, 163–177 (2001).
32. Clauset, A., Shalizi, C. R. & Newman, M. E. Power-law distributions in empirical data. *SIAM Rev.* **51**, 661–703 (2009).
33. Latora, V. & Marchiori, M. Vulnerability and protection of infrastructure networks. *Phys. Rev. E* **71**, 015103 (2005).
34. Viles, W., Ginestet, C. E., Tang, A., Kramer, M. A. & Kolaczyk, E. D. Percolation under noise: detecting explosive percolation using the second-largest component. *Phys. Rev. E* **93**, 052301 (2016).
35. da Silva, C. R., Lyra, M. L. & Viswanathan, G. M. Largest and second largest cluster statistics at the percolation threshold of hypercubic lattices. *Phys. Rev. E* **66**, 056107 (2002).
36. Barabási, A.-L. & Albert, R. Emergence of scaling in random networks. *Science* **286**, 509–512 (1999).
37. Girvan, M. & Newman, M. E. Community structure in social and biological networks. *Proc. Natl Acad. Sci. USA* **99**, 7821–7826 (2002).
38. Motter, A. E., Zhou, C. S. & Kurths, J. Enhancing complex-network synchronization. *Europhys. Lett.* **69**, 334–340 (2005).
39. De Domenico, M., Nicosia, V., Arenas, A. & Latora, V. Structural reducibility of multilayer networks. *Nat. Commun.* **6**, 1–9 (2015).
40. WorldPop, *Migration flows*, <https://www.worldpop.org/geodata/summary?id=1282> (2016). Accessed 10 February 2020.
41. Sorichetta, A. et al. Mapping internal connectivity through human migration in malaria endemic countries. *Sci. Data* **3**, 160066 (2016).
42. Brown, J. A., Rudie, J. D., Bandrowski, A., Van Horn, J. D. & Bookheimer, S. Y. The ucla multimodal connectivity database: a web-based platform for brain connectivity matrix sharing and analysis. *Front. Neuroinf.* **6**, 28 (2012).
43. Brockmann, D. & Helbing, D. The hidden geometry of complex, network-driven contagion phenomena. *Science* **342**, 1337–1342 (2013).

Acknowledgements

The authors thank Dirk Brockmann for providing us with the worldwide air-transportation flow data.

Author contributions

G.B. performed the theoretical analysis, the numerical experiments, the data analysis, and wrote the paper. R.G. performed the numerical experiments and wrote the manuscript. M.D.D. conceived and designed the study and wrote the manuscript.

Competing interests

The authors declare no competing interests.

Additional information

Supplementary information The online version contains supplementary material available at <https://doi.org/10.1038/s42005-021-00612-5>.

Correspondence and requests for materials should be addressed to G.B. or M.D.D.

Reprints and permission information is available at <http://www.nature.com/reprints>

Publisher's note Springer Nature remains neutral with regard to jurisdictional claims in published maps and institutional affiliations.



Open Access This article is licensed under a Creative Commons Attribution 4.0 International License, which permits use, sharing, adaptation, distribution and reproduction in any medium or format, as long as you give appropriate credit to the original author(s) and the source, provide a link to the Creative Commons license, and indicate if changes were made. The images or other third party material in this article are included in the article's Creative Commons license, unless indicated otherwise in a credit line to the material. If material is not included in the article's Creative Commons license and your intended use is not permitted by statutory regulation or exceeds the permitted use, you will need to obtain permission directly from the copyright holder. To view a copy of this license, visit <http://creativecommons.org/licenses/by/4.0/>.

© The Author(s) 2021